OUKA
The University of Osaka
Institutional Knowledge Archive

Title	Reversible modulation of the local environment around metal centers bearing multifunctional carbenes
Author(s)	Yamauchi, Yasuhiro; Ogoshi, Sensuke; Uetake, Yuta et al.
Citation	Chemistry Letters. 2024, 53(3), p. upae042
Version Type	VoR
URL	https://hdl.handle.net/11094/98569
rights	This article is licensed under a Creative Commons Attribution 4.0 International License.
Note	

The University of Osaka Institutional Knowledge Archive : OUKA

https://ir.library.osaka-u.ac.jp/

The University of Osaka

Chemistry Letters, 2024, **53**, upae042
https://doi.org/10.1093/chemle/upae042
Advance access publication 7 March 2024

Highlight Review

Reversible modulation of the local environment around metal centers bearing multifunctional carbenes

Yasuhiro Yamauchi[1], Sensuke Ogoshi[1], Yuta Uetake[1,2,*], Yoichi Hoshimoto[1,3,*]

[1]Department of Applied Chemistry, Faculty of Engineering, Osaka University, 2-1 Yamada-oka, Suita, Osaka 565-0871, Japan

[2]Innovative Catalysis Science Division, Institute for Open and Transdisciplinary Research Initiatives (ICS-OTRI), Osaka University, 2-1 Yamada-oka, Suita, Osaka 565-0871, Japan

[3]Center for Future Innovation (CFi), Division of Applied Chemistry, Faculty of Engineering, Osaka University, 2-1 Yamada-oka, Suita, Osaka 565-0871, Japan

*Corresponding authors: Department of Applied Chemistry, Faculty of Engineering, Osaka University, 2-1 Yamada-oka, Suita, Osaka 565-0871, Japan; Innovative Catalysis Science Division, Institute for Open and Transdisciplinary Research Initiatives (ICS-OTRI), Osaka University, 2-1 Yamada-oka, Suita, Osaka 565-0871, Japan; Center for Future Innovation (CFi), Division of Applied Chemistry, Faculty of Engineering, Osaka University, 2-1 Yamada-oka, Suita, Osaka 565-0871, Japan. Email: uetake@chem.eng.osaka-u.ac.jp, hoshimoto@chem.eng.osaka-u.ac.jp

Abstract

This *Highlight Review* provides examples of external-stimuli-driven reversible modulations of the spatial, electronic, and magnetic environment around metal centers that bear multifunctional *N*-heterocyclic carbenes (NHCs). In particular, recent reports on Lewis-base- or Lewis-acid-mediated reversible molecular transformations of Ni(0) complexes that bear *N*-phosphine-oxide-substituted imidazolylidenes (PoxIms) and the corresponding imidazolinylidenes (SPoxIms) are spotlighted. We also discuss the utility of using X-ray absorption spectroscopy to examine the synthesized (S)PoxIm–Ni complexes to gain spectroscopic insight into the changes in the local environment and electronic state of the metal centers induced by these reversible transformations. Overall, this review highlights the multipurpose utility of multifunctional NHCs as a key to designing and reversibly modulating the local environment of metal centers, which paves the way for accomplishing hitherto challenging molecular transformations and developing unprecedented reactivity of multimetallic compounds.

Keywords: *N*-heterocyclic carbene, nickel complex, X-ray absorption spectroscopy in organic solvents.

Graphical Abstract

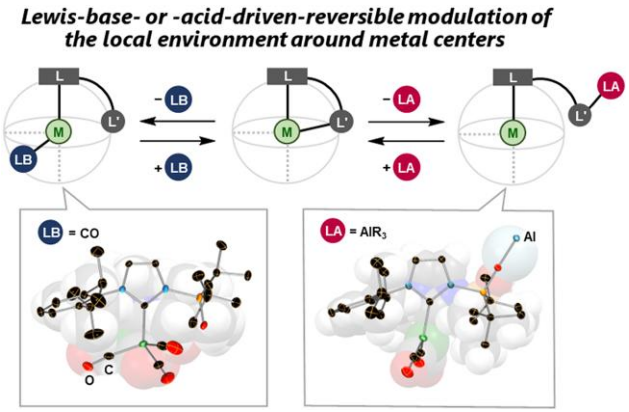

This *Highlight Review* provides examples of external-stimuli-driven reversible modulations of the spatial, electronic, and magnetic environment around metal centers that bear multifunctional *N*-heterocyclic carbenes. In particular, recent reports on Lewis-base- or Lewis-acid-mediated reversible molecular transformations of Ni(0) complexes that bear *N*-phosphine-oxide-substituted imidazolylidenes and the corresponding imidazolinylidenes are spotlighted.

Designing and modulating the local spatial and electronic environment of metal centers in organometallic complexes is a critical research subject in the fields of homogeneous catalysis,[1–6] supramolecular chemistry,[7,8] and materials science.[9] So far, chemists have dedicated much attention to the structural and electronic properties of supporting ligands,[10] and ligands that can undergo reversible structural and electronic changes are commonly applied in redox,[11,12] photoexcitation,[6,13–15] and protonation[16] processes. Moreover, multifunctional ligands that undergo conformational isomerization in response to an external stimulus can drastically modify the spatial environment around the metal center and hence enhance or dampen the reactivity of the organometallic complexes through modulation of the volume and shape of the available reaction field.[17–19] Achieving such spatial modulation in a reversible and (nearly) quantitative manner often requires a judicious combination of the external stimuli, metals, and functional groups of the ligands. For example, reversible ligand-substitution processes through the dissociation of L′ in the presence of an external Lewis base (LB) have already been reported (Fig. 1, left; L′ = hemilabile

[Received on 16 February 2024; revised on 4 March 2024; accepted on 4 March 2024; corrected and typeset on 26 March 2024]
© The Author(s) 2024. Published by Oxford University Press on behalf of the Chemical Society of Japan.
This is an Open Access article distributed under the terms of the Creative Commons Attribution License (https://creativecommons.org/licenses/by/4.0/), which permits unrestricted reuse, distribution, and reproduction in any medium, provided the original work is properly cited.

Downloaded from https://academic.oup.com/chemlett/article/53/3/upae042/7623711 by USACO ref BMB 39121 user on 06 December 2024

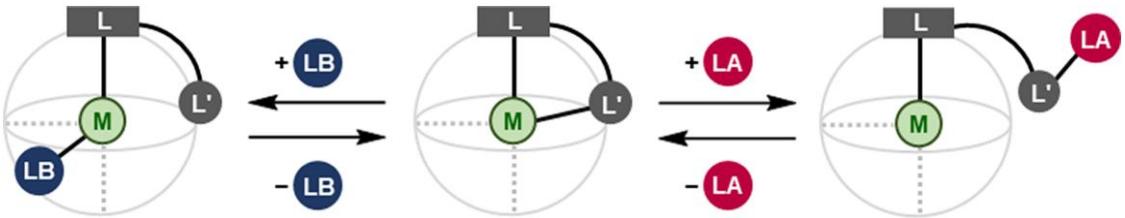

Fig. 1. Simplified scheme of the reversible modulation of the spatial and electronic environment around a metal center in an organometallic complex mediated by a Lewis base (LB, left) or Lewis acid (LA, right).

coordination moieties).[20–24] On the other hand, strategies based on the use of Lewis acids (LAs) remain underdeveloped (Fig. 1, right), possibly due to the difficulty in preventing irreversible decomposition of the organometallic complex through the abstraction of the supporting L (shown in Fig. 1) by the LA and/or the formation of equilibrium mixtures that are difficult to separate. Thus, the demonstration of such an LA-mediated process as a conceptually novel strategy to design and reversibly modulate the local environment in transition-metal complexes that bear multifunctional ligands would be noteworthy.

Multifunctional *N*-heterocyclic carbenes (NHCs), i.e. NHCs with at least one functional group in addition to the carbene moiety, are a promising tool for modulating the local environment of metal centers given the high stability of NHC-ligated complexes and the availability of a wide range of additional functional groups that can play a critical role as the external-stimulus-responsive units.[9,25,26] Multifunctional NHCs with a variety of L′ moieties, e.g. phosphine,[27] phosphine oxide,[24,28] amine,[29] thioether,[30] and alkoxy[31] groups, on the nitrogen atoms have already been synthesized and used as ligands for transition-metal-based catalysts and functional materials based on the specific reactivity of the hemilabile L′. Our group has also reported the synthesis and reactivity of *N*-phosphine-oxide-substituted imidazolylidenes (PoxIms) and the corresponding imidazolinylidenes (SPoxIms) (Fig. 2a).[25,26] (S)PoxIms include 2 distinct Lewis-basic functions, i.e. the hard phosphine-oxide moiety and the relatively soft carbene moiety. The (S)PoxIms undergo conformational isomerization between their *syn*- and *anti*-conformers (defined by the relative orientation of the carbene and oxygen atoms with respect to the N–P bonds) via rotation of the *N*-phosphinoyl groups. We found that the *anti*-conformers are energetically more favorable than the *syn*-conformers, whereas the rotation of the *N*-phosphinoyl groups can take place easily at room temperature.[25] The hemilabile and dynamic reactivity of the *N*-phosphinoyl groups in (S)PoxIms enables the formation of a variety of transition-metal complexes (Fig. 2b). For example, the complexation takes place between an equimolar amount of (S)PoxIm and group-10 metals such as Ni and Pd in a *syn*-*κ*-*C*,*O*[24,28] or *syn*-*κ*-*C*[32] fashion to afford tetrahedral and trigonal-planar complexes, depending on the reaction conditions. On the other hand, group-11 metals such as Cu[19] and Au[32] form *anti*-(S)PoxIm complexes in a *κ*-*C* fashion given their characteristic propensity to adopt 2-coordinated linear geometries; in such complexes, the reaction field around the carbene atoms is significantly limited by the sterically demanding ^{t}Bu groups. Recently, we have demonstrated that (S)PoxIms can serve as a platform for the formation of heterobimetallic (Cu/Al[19] and Ni/Al[33]) complexes based on the high affinity of organoaluminum(III) species.

Against this background, this review highlights strategies to reversibly modulate the local environment (i.e. the spatial, electronic, and magnetic environment) around metal centers that bear multifunctional (S)PoxIm ligands through the use of external LBs and LAs. In particular, we summarize the following two reports: (i) the interconversion between Ni(*κ*-*C*,*O*-(S)PoxIm)

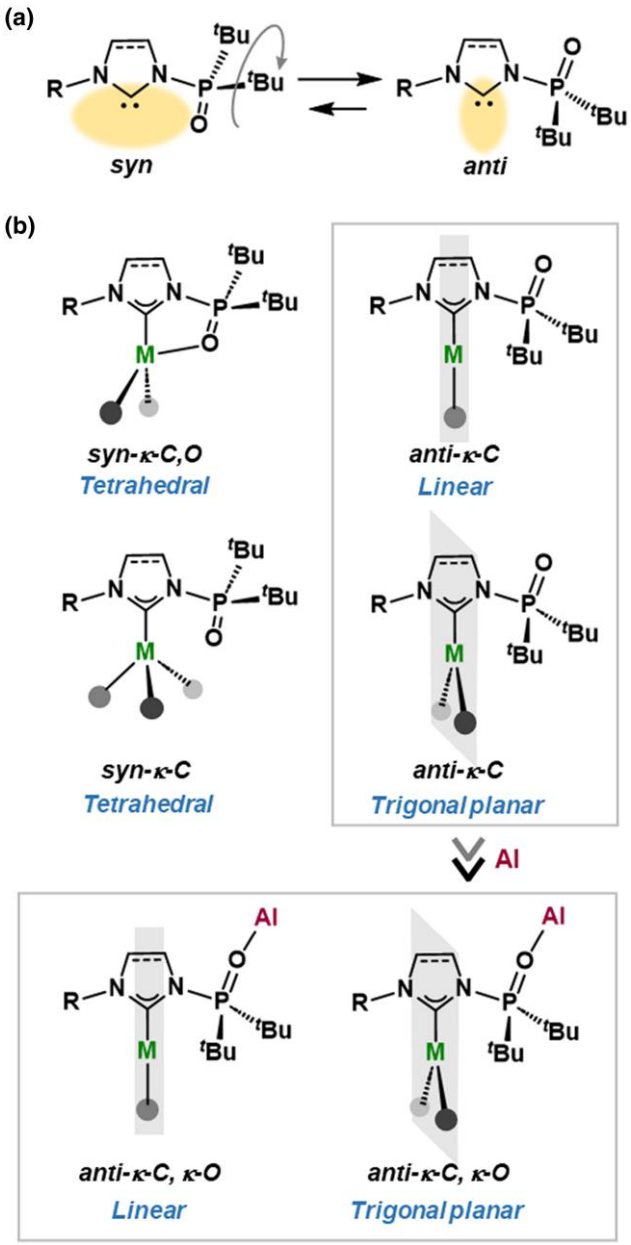

Fig. 2. a) Interconversion between the *syn*- and *anti*-conformers of (S)PoxIms. b) Examples of hitherto reported coordination modes of (S)PoxIms in mono- and bimetallic transition-metal complexes. M = Ni, Cu, Pd, Au.

Downloaded from https://academic.oup.com/chemlett/article/53/3/upae042/7623711 by USACO ref BMB 39121 user on 06 December 2024

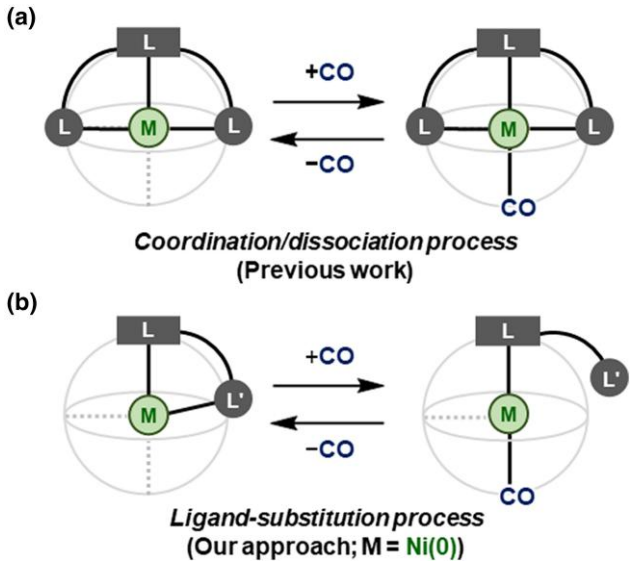

Fig. 3. Comparison of the design strategies between a) previously reported systems using high-valent metals and b) the Ni(0)-based arrangement in our system.

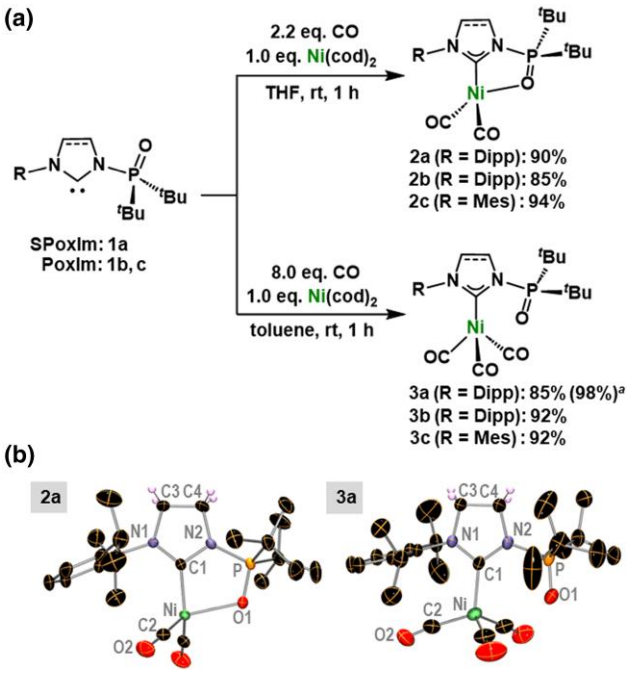

Fig. 4. a) Selective preparation of Ni(κ-*C,O*-**1**)$(CO)_2$ (**2**) and Ni(κ-*C*-**1**)$(CO)_3$ (**3**). [a]^{1}H NMR yield confirmed *in situ*. b) Molecular structures of **2a** and **3a** with thermal ellipsoids at 30% probability; H atoms (except those on C3 and C4) are omitted for clarity.

$(CO)_2$ and Ni(κ-C-(S)PoxIm)$(CO)_3$ through the coordination/dissociation of CO, which has already been applied for the development of a room-temperature pressure-swing reversible chemisorption system on Ni(0); and (ii) the interconversion between Ni(κ-C,O-(S)PoxIm)$(CO)_2$ and {κ-C-Ni$(CO)_2$}(μ-*anti*-(S)PoxIm){κ-O-Al$(C_6F_5)_3$} through complexation-induced rotation of the *N*-phosphinoyl moieties using $Al(C_6F_5)_3$. In addition, this *Highlight Review* also focuses on the evaluation of the local environment around the metal centers based on single-crystal X-ray diffraction (SC-XRD) and X-ray absorption spectroscopy (XAS).

1. Reversible chemisorption of carbon monoxide on nickel(0) complexes

CO plays an essential role as a C1 feedstock in the contemporary production of value-added chemicals. Huge amounts of high-purity CO are produced during the removal of contaminants such as H_2, N_2, CO_2, and CH_4 from crude materials obtained from the gasification of hydrocarbon resources[34] and the steel-production industry.[35] Our group has envisioned a conceptually novel approach for the reversible chemisorption of CO using low-valent transition-metal complexes, as their high CO affinity can be expected to ensure rapid and efficient adsorption of CO and hence form the basis of a useful removal system. However, the dissociation of CO from low-valent late-transition-metal centers is known to be sluggish, as exemplified by the Mond process, which requires the thermolysis of gaseous $Ni(CO)_4$ at 180 to 280 °C.[36,37] Thus, the hitherto reported adsorption technologies mainly rely on the chemisorption of CO by coordinatively unsaturated higher-valent metals to minimize the influence of metal-to-CO π-backdonation (Fig. 3a).[38,39] In this context, we hypothesized that reversible CO chemisorption could be achieved on Ni(0) through intramolecular ligand-substitution mechanisms enabled by hemilabile (S)PoxIm ligands under pressure-swing conditions (Fig. 3b).

First, we explored the preparation of Ni carbonyl complexes that bear (S)PoxIms. Treatment of a tetrahydrofuran (THF) solution of SPoxIm **1a** and $Ni(cod)_2$ (cod = 1,5-cyclooctadiene) with 2.2 equiv. of *ex situ*-generated CO resulted in the formation of Ni(κ-C,O-**1a**)$(CO)_2$ (**2a**), which was isolated in 90% yield (Fig. 4a). On the other hand, the use of excess CO (~8.0 eq.) at room temperature in toluene resulted in the selective preparation of Ni(κ-C-**1a**)$(CO)_3$ (**3a**), which was isolated in 85% yield. It is noteworthy here that these results represented the first demonstration of the selective formation of Ni(0) complexes that bear two or three carbonyl ligands in the presence of a single NHC ligand. Di-/tricarbonyl complexes **2b**/**3b** and **2c**/**3c** were prepared in a similar manner. These compounds were unambiguously characterized using multinuclear NMR and infrared (IR) absorption spectroscopy as well as single-crystal X-ray diffraction (SC-XRD) analyses (Fig. 4b). The A_1-symmetrical carbonyl stretching vibrations of **3a**–**c** (2,048 to 2,049 cm^{-1}; in CH_2Cl_2)[24,40] are slightly lower than those of Ni(κ-C-**1d**/**1e**)$(CO)_3$ (**3d**/**3e**, 2,052 cm^{-1}),[41] where **1d** is 1,3-bis(2,6-diisopropylphenyl)imidazolidin-2-ylidene and **1e** is 1,3-bis(2,6-diisopropylphenyl)imidazol-2-ylidene, indicating a negligible difference in the electron density on their Ni(0) centers.[24]

Upon concentrating a toluene solution of **3a** *in vacuo* at room temperature, we observed the partial formation of **2a**, which confirmed the viability of our ligand-substitution strategy. In fact, stirring the crystalline powder of **3a** at room temperature for 10 h *in vacuo* (0.3 mmHg) resulted in the formation of **2a** in 50% yield (Fig. 5). To promote the desorption of the CO ligands, we explored the use of a dispersant or solvent to increase the area exposed to the reduced pressure. Dispersing **3a** into tetradecane ($C_{14}H_{30}$) in the reaction flask resulted in a significant improvement in the desorption, i.e. **2a** was obtained in >99% yield after 2 h of stirring at room temperature, which was accompanied by loss of crystallinity. Desorption also proceeded quantitatively within 30 min when **3a** was fully dissolved in 1,3-dimethoxybenzene (DMB). However, we also confirmed the partial (~2 wt%) removal of $C_{14}H_{30}$ or DMB under the

Downloaded from https://academic.oup.com/chemlett/article/53/3/upae042/7623711 by USACO ref BMB 39121 user on 06 December 2024

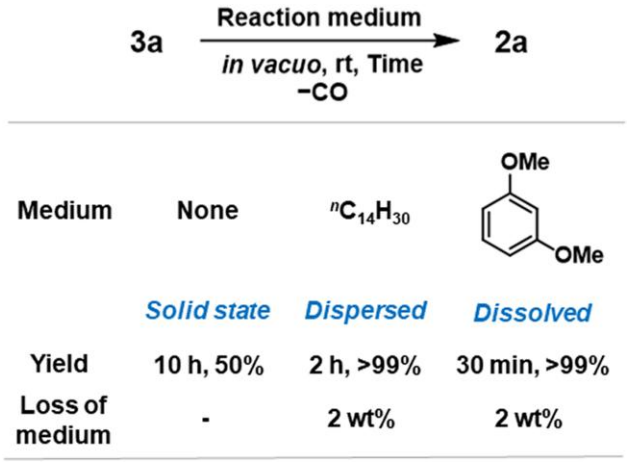

Medium	None	$^{n}C_{14}H_{30}$	
	Solid state	Dispersed	Dissolved
Yield	10 h, 50%	2 h, >99%	30 min, >99%
Loss of medium	-	2 wt%	2 wt%

Fig. 5. Effect of dispersants on the desorption of CO from **3a**.

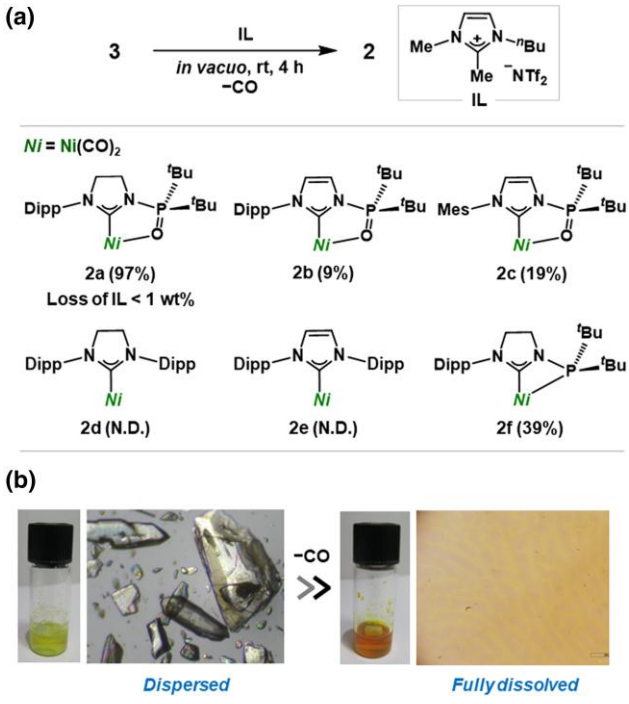

Fig. 6. Desorption of CO from **3** in **IL**. a) Effect of the ligand. b) Photographs and micrographs of reaction samples during CO desorption from **3a** to give **2a**.

applied reduced pressure conditions, which should be avoided to achieve a fully reusable and reversible chemisorption system.

We reasoned that the use of ionic liquids, which exhibit negligible vapor pressure, might solve the medium-loss problem. The dispersion of a crystalline-powder sample of **3a** in an imidazolium-based **IL** with the $[N(SO_2CF_3)_2]^-$ (NTf_2^-) anion under reduced pressure at room temperature for 4 h resulted in the formation of **2a** in 97% yield, and the loss of **IL** after the desorption period was negligible (Fig. 6a). It should also be noted here that a significant amount of crystalline **3a** was dispersed in the **IL** during the initial stage of the CO desorption, whereas a nearly homogeneous solution was observed after the reaction had completed due to the sufficient solubility of **2a** in the **IL** (Fig. 6b).

On the other hand, **3b** showed only 9% desorption of CO, even though the geometric and electronic features of **3a** and **3b** are

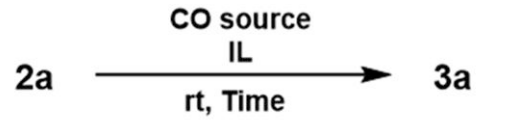

CO source	
CO/N_2 (1 atm each)	98%, 15 min
$CO/CH_4/N_2$ (1 atm each)	89%, 30 min
$CO/H_2/N_2$ (1 atm each)	86%, 30 min

Fig. 7. Adsorption of CO by **2a** in **IL**.

almost identical (*vide supra*). This result should most likely be interpreted in terms of the different structural flexibility of the saturated and unsaturated backbone framework in **1a** and **1b**, respectively. Complex **3c** was also subjected to identical desorption conditions, but the resulting yield of **2c** was only 19%. No reaction occurred for **3d** and **3e**. To evaluate the role of the *N*-phosphinoyl oxygen atom in **3a**, we synthesized Ni(*κ*-*C*-**1f**)$(CO)_3$ (**3f**), where **1f** is a *N*-phosphanyl-substituted imidazolidin-2-ylidene; **3f** underwent desorption of CO to generate Ni(*κ*-*C*,*P*-**1f**)$(CO)_2$ (**2f**) in 39% yield. These results demonstrate that the hemilabile behavior of the *N*-phosphinoyl moiety and the structural flexibility derived from the ethylene moiety in the imidazolidine-2-ylidene ring are both essential for an efficient desorption of CO from the Ni(0) center under the applied conditions.

We then investigated the adsorption of CO by **2** in the presence of **IL** at room temperature (Fig. 7). Stirring **2a** in **IL** under a CO/N_2 (1 atm each) atmosphere afforded **3a** in 98% yield via the selective adsorption of CO accompanied by precipitation of small crystals of **3a**. In addition, CO was directly stored in **3a** through adsorption by **2a** from gaseous mixtures of $CO/CH_4/N_2$ (1 atm each) and $CO/H_2/N_2$ (1 atm each) in excellent yield. Thus, the present system can also be used for the purification of CH_4 and H_2 through removal of the accompanying CO.

Subsequently, we investigated the reusability of the Ni(0)-based chemisorption system (Fig. 8). Complex **2a** was afforded in 87 to 88% yield within 2 h using a sample of **3a** that had been prepared under the optimized conditions via either the adsorption of CO on **2a** or sequential CO desorption–adsorption reactions from a crystalline sample of **3a**. However, when a larger crystal of **3a**, obtained by recrystallization from toluene/*n*-hexane at −30 °C, was used, **2a** was obtained in only 67% yield. This is probably due to the increased surface area of **3a**, as the crystals of **3a** that were reprecipitated after CO adsorption were significantly smaller than those used in the first desorption process. Importantly, CO was effectively desorbed from **3a** even after five desorption–adsorption cycles.

2. Reversible modulation of the local environment around nickel(0) centers via $Al(C_6F_5)_3$-induced conformational isomerization of (S)PoxIm ligands

LAs represent a potential trigger for the reversible modulation of the spatial environment around metal centers with

Downloaded from https://academic.oup.com/chemlett/article/53/3/upae042/7623711 by USACO ref BMB 39121 user on 06 December 2024

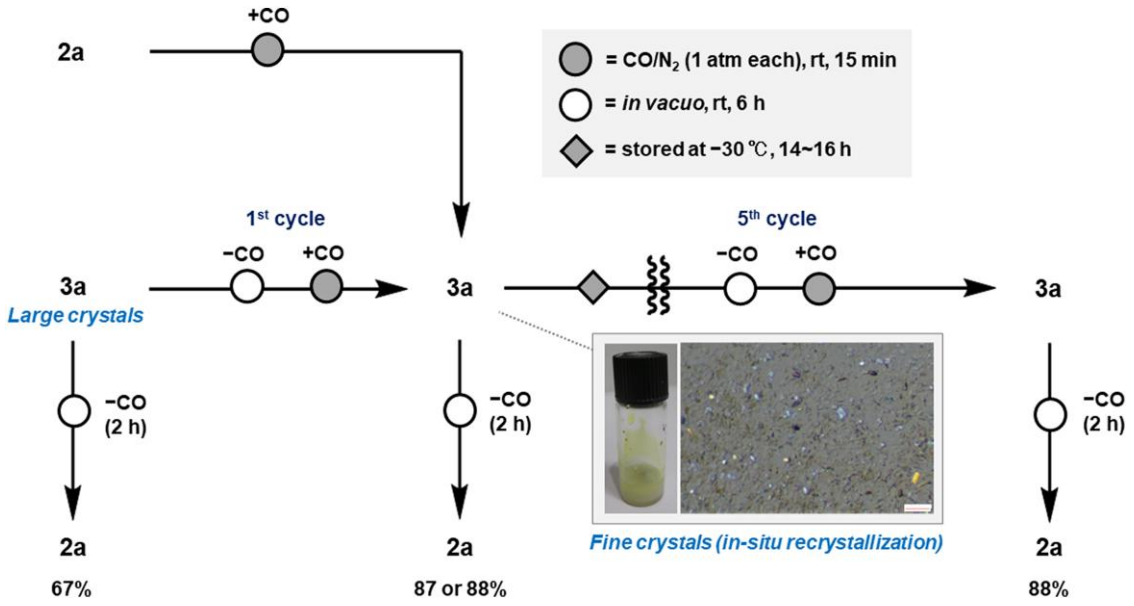

Fig. 8. Repeated use of the developed CO-chemisorption system. The shown scale bar is equivalent to 3.0 mm.

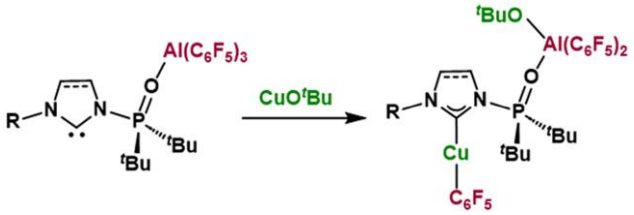

Fig. 9. Formation of Cu/Al heterobimetallic complexes that bear (S) PoxIms.

multifunctional ligands.[7,8] However, examples of such LA-mediated reactions have often been limited due to the difficulty in finding a suitable combination of multifunctional ligands and LAs. In this context, a conceptually similar approach has been reported by Fan et al., who used host–guest interactions between Na^+ and crown–ether moieties introduced in a Rh complex that bears Aza-CrownPhos to achieve the reversible regulation of the coordination environment and reactivity of the Rh catalyst through the addition/removal of Na^+.[18]

We envisioned that an LA-mediated reversible modulation of the local environment around the metal centers shown in Fig. 1 could potentially be achieved based on interconversion between a monometallic species bearing *syn*-(S)PoxIm and a heterobimetallic species bearing *anti*-(S)PoxIm. For this purpose, an isolable (or at least spectroscopically observable) complex should be generated with the sterically demanding *anti*-(S)PoxIm ligands. Moreover, the metal center should undergo the geometric transformation reversibly through the coordination/dissociation of the *N*-phosphinoyl moieties. Initially, we explored the complexation between *anti*-(*κ*-*O*-(S)PoxIm)$Al(C_6F_5)_3$ and CuO^tBu and observed the formation of {*κ*-*C*-$Cu(C_6F_5)$}(*κ*-*anti*-(S)PoxIm){*κ*-*O*-$Al(C_6F_5)_2(O^tBu)$} via an irreversible intramolecular Cu–O^tBu/Al–C_6F_5 transmetalation triggered by the rotation of the *N*-phosphinoyl moiety (Fig. 9).[19] This result demonstrated that the rotation of the *N*-phosphinoyl moiety in (S)PoxIms can play a critical role in preprogramming the encounter of the two organometallic fragments in the heterobimetallic complex; however, creating a system that could reversibly modulate the local environment around the metal centers remained challenging. We thus turned our attention to the use of Ni(0) complex based on the preparation of trigonal-planar Ni(0) dicarbonyl complexes that bear bulky NHCs such as (I^tBu)$Ni(CO)_2$ and (IAd)$Ni(CO)_2$ (I^tBu = 1,3-di-*tert*-butylimidazol-2-ylidene; IAd = 1,3-di-adamantylimidazol-2-ylidene).[42]

We first examined the reaction between tetrahedral **2a** and an equimolar amount of $Al(C_6F_5)_3(tol)_{0.5}$, which resulted in the selective formation of heterobimetallic Ni/Al complex **4a** in 90% yield (Fig. 10a). We also confirmed that the $Al(C_6F_5)_3$-mediated rotation of the *N*-phosphinoyl moieties in **2b/2c** afforded the corresponding heterobimetallic Ni/Al complexes **4b/4c** with trigonal-planar geometry in good-to-high yield. The molecular structure of **4a** obtained from the SC-XRD analysis is shown in Fig. 10c. The participation of an anagostic interaction between Ni and C5–H was corroborated by using theoretical calculations. Subsequently, we treated **4a** with a slight excess of 4-dimethylaminopyridine (DMAP) and confirmed the quantitative regeneration of **2a** with concomitant formation of the adduct DMAP–$Al(C_6F_5)_3$ (Fig. 10b).

We confirmed that this strategy can be expanded to (*syn*-*κ*-*C*,*O*-**1a**)Ni complex **5a**, which features an η^2:η^2-diphenyldivinylsilane ligand instead of CO ligands (Fig. 11a). Treatment of **5a** with $Al(C_6F_5)_3(tol)_{0.5}$ resulted in the quantitative formation of heterobimetallic Ni/Al complex **6a** via the complexation-induced rotation of the *N*-phosphinoyl moiety. Moreover, the addition of DMAP caused again the dissociation of $Al(C_6F_5)_3$ to regenerate **5a**. We found that the ^{1}H NMR resonances of the coordinated olefin moieties, which are magnetically equivalent in solution at room temperature, shifted upfield upon changing in coordination around the Ni center from tetrahedral in **5a** to distorted trigonal planar in **6a** (Fig. 11b). These results suggest that the $Al(C_6F_5)_3$-mediated rotation of the *N*-phosphinoyl group can modulate not only the spatial environment around the Ni center, but also the magnetic environment surrounding the coordinated 1,4-diene unit, through the interconversion between **5a** and **6a**.

Downloaded from https://academic.oup.com/chemlett/article/53/3/upae042/7623711 by USACO ref BMB 39121 user on 06 December 2024

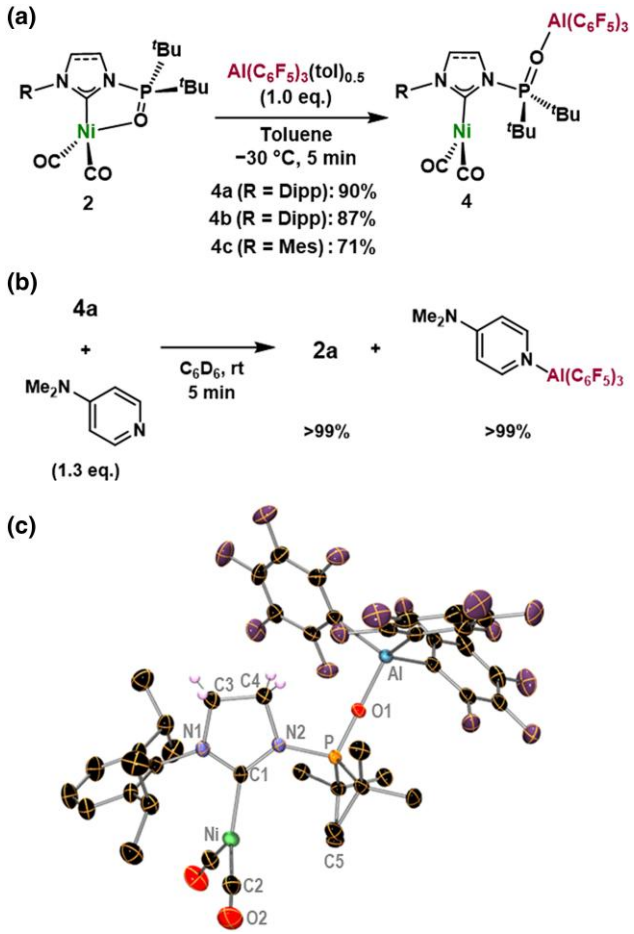

Fig. 10. a) Synthesis of the heterobimetallic Ni/Al complexes **4**. b) Reaction of **4a** with DMAP. c) Molecular structure of **4a** with thermal ellipsoids at 30% probability; H atoms (except those on C3 and C4) are omitted for clarity.

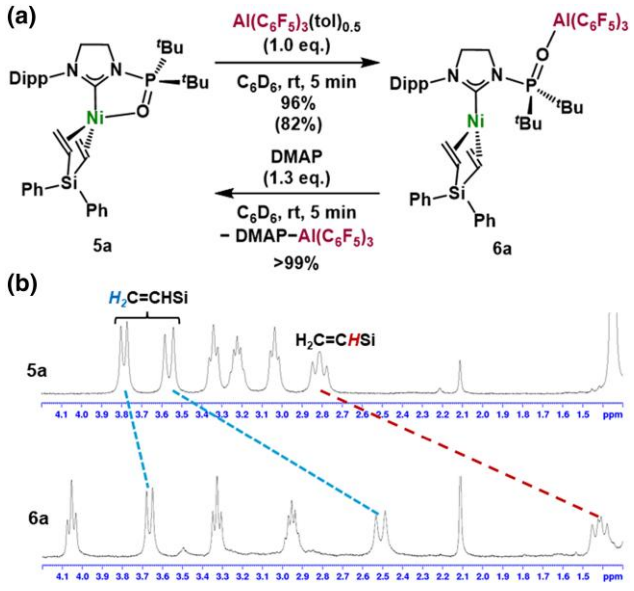

Fig. 11. a) Interconversion between **5a** and **6a** mediated by $Al(C_6F_5)_3$. The yield was determined by using ^1H NMR analysis. The yield of isolated products is shown in parentheses. b) ^1H NMR spectra of **5a** and **6a**.

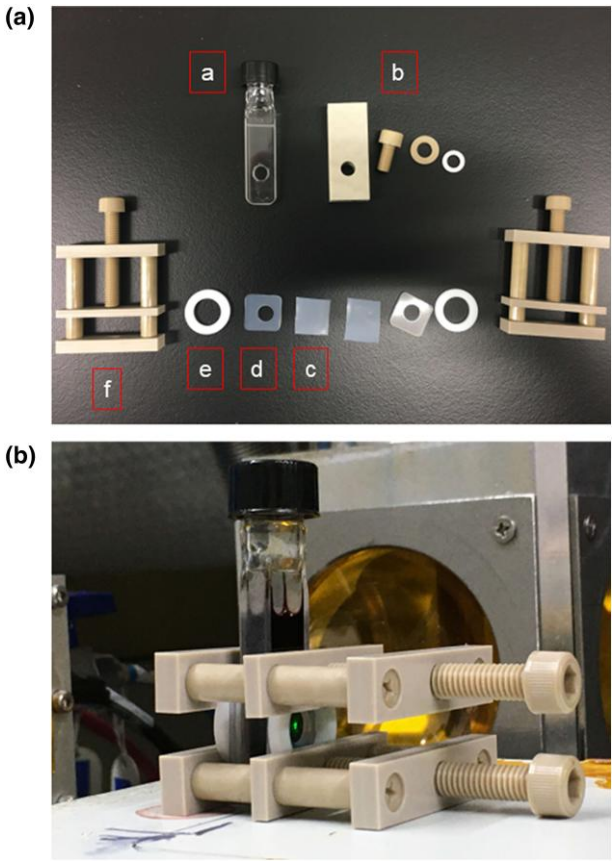

Fig. 12. Custom-built solution cell for XAS. a) Disassembled cell. (a) Borosilicate glass cell. (b) PEEK cell. (c) PTFE windows (50 μm thickness). (d) Silicon rubber sheets with a ϕ6 mm hole (15 mm × 15 mm × 1.5 mm). The silicon rubber sheets were handcrafted by using die-cutting with hole-punching tools. (e) PTFE packings. (f) PEEK pinchcocks. b) The final setup.

3. XAS of nickel complexes

XAS is a powerful method for analyzing the electronic structure and coordination environment of target elements, and has a wide range of applications in various scientific disciplines, including materials science, chemistry, and biology.[43–47] Unlike other techniques for investigating the electronic state, such as X-ray photoelectron spectroscopy, XAS does not require high-vacuum conditions when hard X-rays (>4 keV) are used, which allows XAS to be performed on most transition-metal complexes in aqueous and organic solvents. Recently, solution-phase XAS analysis has gained substantial attention in organometallic chemistry as a means to observe reaction intermediates in homogeneous catalytic reactions and the solution-state behavior of metal complexes.[48–60] We have also developed custom-built solution cells that are applicable for XAS in organic solvents and used them to perform XAS analysis on (S)PoxIm–Ni systems at synchrotron facilities in Japan, such as SPring-8 and the Photon Factory (PF).[24,33] As shown in Fig. 12a, the custom-built solution cell is composed of a borosilicate glass (a) or a polyetheretherketone (PEEK) (b) body with a hole drilled through it to ensure high organic solvent tolerance. The cell body is sandwiched between 50 μm polytetrafluoroethylene (PTFE) sheet windows (c), silicone rubber sheets (d), PTFE O-rings (e), and PEEK pinchcocks (f) to fabricate a solution cell (Fig. 12b). We have not observed any leakage of the

Downloaded from https://academic.oup.com/chemlett/article/53/3/upae042/7623711 by USACO ref BMB 39121 user on 06 December 2024

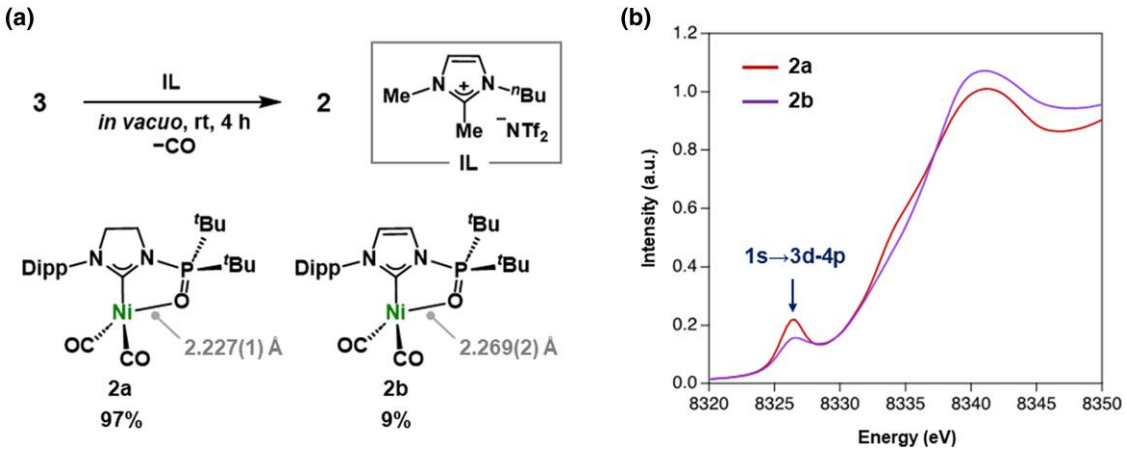

Fig. 13. a) Desorption of CO from **3a** and **3b** in **IL**. b) Ni K-edge XAS spectra of **2a** and **2b**.

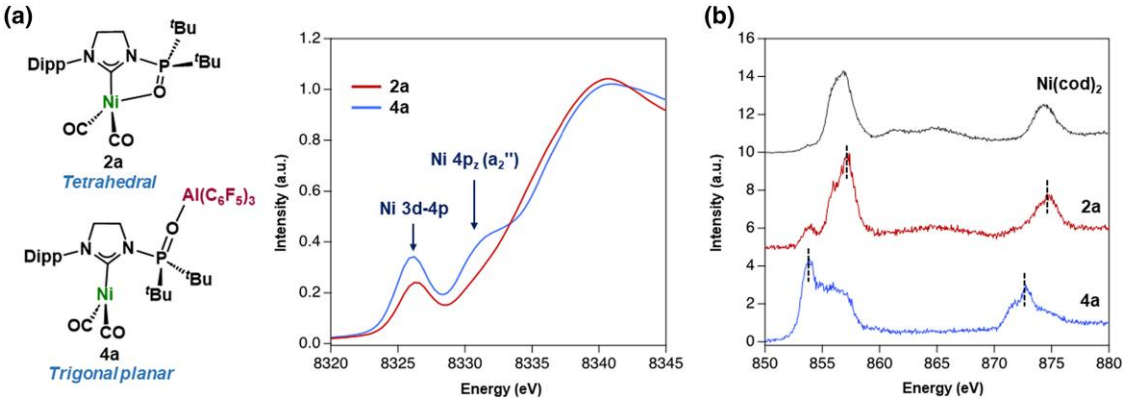

Fig. 14. a) Ni K- and b) $L_{2,3}$-edge XAS spectra of **2a** and **4a**.

solvent during XAS experiments, even when highly corrosive organic solvents, such as THF and *N*,*N*-dimethylformamide (DMF), are used. Moreover, we do not use expensive consumables such as silicon nitrogen membranes, which significantly reduces the initial and running costs for the solution-state XAS experiments.

One difficulty in interpreting the XAS data of transition-metal complexes with multiple ligands is that both electronic and structural factors affect the spectrum. Therefore, it is sometimes difficult to extract the structure–spectrum relationships, which renders a clear understanding of XAS data difficult. In this context, our series of (S)PoxIm–Ni complexes provides an ideal system for studying structure–spectrum relationships in XAS because they adopt a wide variety of coordination modes with minimal change in their ligands, as shown in Fig. 2. Thus, we began our XAS studies using the series of (S)PoxIm–Ni complexes applied in the above-described reversible reactions.

Our study commenced with measuring the solid- and solution-state XAS of nickel dicarbonyl complexes to examine the ligand effect on the CO-desorption process (Fig. 13a). The Ni K-edge XAS analysis was performed using the transmission method at the SPring-8 BL14B2 beamline, and all solid and solution samples were prepared in a glovebox filled with argon gas. The XAS spectra of nickel dicarbonyl complexes **2a** and **2b** in the solid state, which show the differences between the SPoxIm and PoxIm ligands in the CO-adsorption/-desorption reactions, are presented in Fig. 13b. A pre-edge peak corresponding to the electric dipole transition from the Ni 1s orbital to the Ni 4p(−3d) orbitals was observed at 8,326 eV and no characteristic peak was detected at the absorption edge, which is typical for nickel complexes with tetrahedral coordination geometry. A substantial difference in the peak intensity of the pre-edge region in the XAS spectra of **2a** and **2b** was observed. Since the pre-edge intensity is strongly related to the displacement from the ideal tetrahedral coordination geometry, which causes the 3d–4p mixing of the nickel center, the higher intensity observed for **2a** could be rationalized in terms of a lower symmetry around the nickel center, which would be caused by the rather flexible imidazolidin-2-ylidene framework. Additionally, SC-XRD analysis indicated that the length of the Ni–O bond in **2a** was 2.227(1) Å, which was shorter than that in **2b** (2.269(2) Å). This can be attributed to the greater structural flexibility derived from the ethylene moiety in the SPoxIm ligand, which allows greater distortion of the structure than the PoxIm ligand; this is also in good agreement with the XAS data. Based on the XAS and SC-XRD results, the flexible SPoxIm ligand can be expected to facilitate the desorption of CO through an intramolecular S_N2-like reaction, thus increasing the efficiency of the desorption of CO from **3** to give **2** (**2a**: 97%, **2b**: 9%).

Subsequently, we carried out an XAS analysis on the (*syn*-*κ*-*C*,*O*-SPoxIm)Ni(CO)$_2$/Al(C$_6$F$_5$)$_3$ system in order to track the changes in the electronic structure upon changing between the tetrahedral and trigonal-planar coordination

Downloaded from https://academic.oup.com/chemlett/article/53/3/upae042/7623711 by USACO ref BMB 39121 user on 06 December 2024

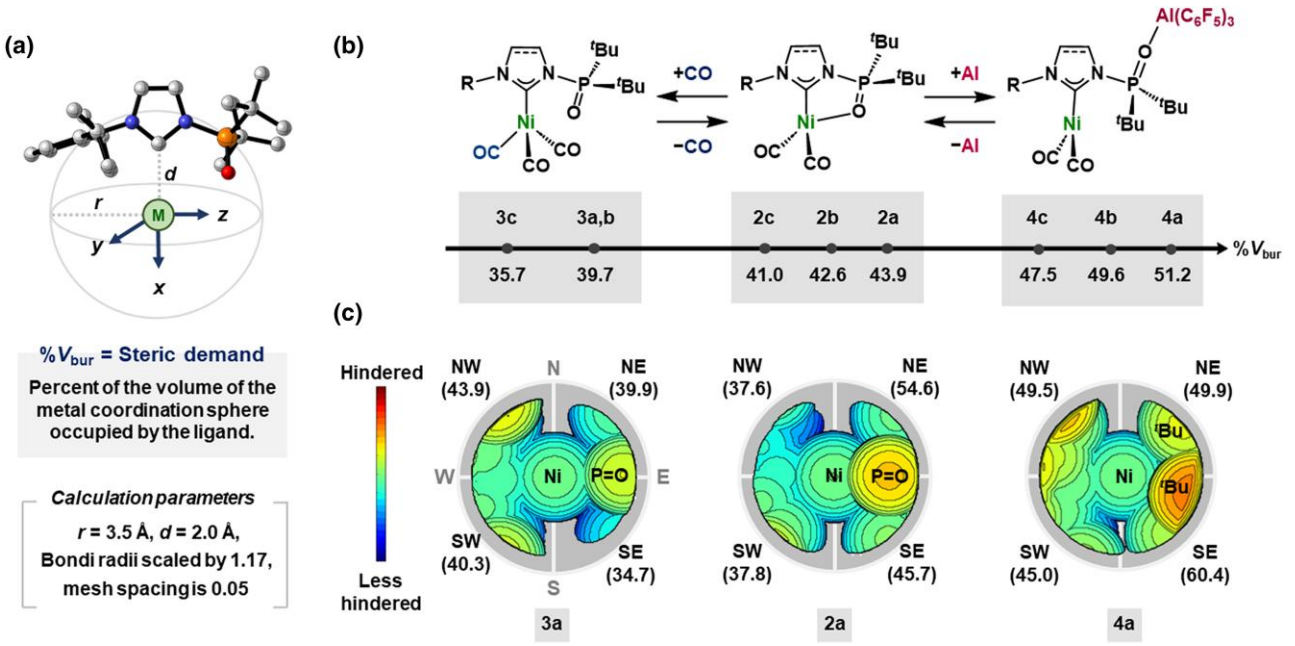

Fig. 15. a) Simplified representation of percent buried volume (%V_{bur}). b) %V_{bur} values of **2a–c**, **3a–c**, and **4a–c**. c) Topographic steric maps of **2a**, **3a**, and **4a**, calculated using Samb*V*ca.

geometries. The Ni K-edge XAS of **2a** and **4a** in toluene is presented in Fig. 14a. In the case of trigonal-planar **4a**, a remarkable peak appeared in the edge region (8,331 eV) and the pre-edge peak intensity (8,326 eV) was greater than that for **2a**. Given that the nonbonding $4p_z$ orbital (a_2'' symmetry) is commonly found in trigonal-planar 16-electron complexes, we attributed the characteristic edge peak to the Ni $1s \rightarrow 4p_z$ transition and the solution-phase XAS results clearly suggest a trigonal-planar geometry of **4a** in toluene. We further explored the electronic structures of the 3d orbitals of **2a** and **4a** based on a Ni $L_{2,3}$-edge XAS analysis in the solid state (Fig. 14b). Given that the L_2- and L_3-edge XAS of 3d transition metals correspond to transitions from the $2p_{1/2}$ and $2p_{3/2}$ orbitals to 3d orbitals, respectively, the $L_{2,3}$-edge XAS contains information on the electronic structure of the unoccupied 3d orbitals, which plays an important role in determining the nature of metal complexes. The Ni $L_{2,3}$-edge XAS analysis was performed using the partial fluorescence yield method at the PF BL-19B beamline. In the cases of **2a** and $Ni(cod)_2$, the absorption maxima of the Ni L_3-edge appear at 856.0 and 856.2 eV, respectively, with a shoulder peak in their lower-energy regions. Their Ni $L_{2,3}$-edge XAS spectra present spectroscopic features characteristic of tetrahedral nickel complexes with a d^{10} electron configuration. In contrast, for **4a**, the peak maximum shifts toward the lower-energy region to 852.9 eV, clearly indicating that the 3d orbitals are stabilized through the formation of the 16-electron complex with a vacant $4p_z$ orbital.

4. Quantitative evaluation of the spatial environment around the nickel center based on the percent buried volume values

Finally, the impact of the *N*-phosphinoyl dissociation/association and rotation on the spatial environment surrounding the Ni center was quantitatively evaluated based on the percent buried volume (%V_{bur}).[2,61] The %V_{bur} value represents the volume occupied by a ligand within the coordination sphere of a metal and, thus, a ligand with a larger %V_{bur} is sterically more demanding than one with a smaller %V_{bur} under identical calculation conditions (Fig. 15a). The %V_{bur} values were calculated based on the geometric parameters of **2**, **3**, and **4** in the crystalline state (Fig. 15b).[24,33] Topographic steric maps visualizing the %V_{bur} values in the northwestern (NW), northeastern (NE), southwestern (SW), and southeastern (SE) quadrants were produced using the Samb*V*ca 2 program (Fig. 15c). The %V_{bur} values increase in the order **3** (35.7 to 39.7) < **2** (41.0 to 43.9) < **4** (47.5 to 51.2), thus clearly demonstrating that the space around the Ni center is significantly altered via the dissociation/coordination as well as the rotation of the *N*-phosphinoyl moiety. The modulation of the shape was also confirmed by comparison of the %V_{bur}(NE) and %V_{bur}(SE) values of **2a**, **3a**, and **4a**. The reported monodentate NHCs yield either nickel dicarbonyl or tricarbonyl complexes, depending on their steric demand, when a single molecule of NHC is treated with a Ni(0) species.[41,42] Interestingly, a %V_{bur} value of 39.7 to 41.0 seems to represent a plausible boundary regarding whether a di- or a tricarbonyl (S)PoxIm–Ni(0) complex is generated as an isolable species. In this context, (S)PoxIms **1a–c** demonstrate unprecedented reactivity to afford both di- and tricarbonyl complexes, and realize their interconversion beyond this possible %V_{bur} threshold.

5. Conclusions

In this *Highlight Review*, we have described our strategy to enable the reversible modulation of the electronic state and spatial environment around metal centers by taking advantage of multifunctional (S)PoxIms ligands. First, we discussed the effective interconversion between the Ni(0)–dicarbonyl and Ni(0)–tricarbonyl complexes in ionic liquids, which was achieved via the reversible ligand substitution of the phosphinoyl group and carbon monoxide as external LBs. This serves as a proof-of-concept for a reusable and reversible Ni(0)-based chemisorption system for CO. Second, the reversible ligand

Downloaded from https://academic.oup.com/chemlett/article/53/3/upae042/7623711 by USACO ref BMB 39121 user on 06 December 2024

dissociation between the phosphinoyl group and the Ni(0) complexes mediated by $Al(C_6F_5)_3$ was described, in which the nickel center adopts a tetrahedral or trigonal-planar coordination geometry without the formation of quenched LB–LA adducts. During our studies, we developed liquid cells for XAS in organic solvents and unveiled the solution-state structure and behavior of a series of (S)PoxIm–Ni complexes. Eventually, a detailed discussion of the XAS and $\%V_{bur}$ values shed light on the changes in the electronic and spatial environment around the Ni centers. Thus, this work manifests a conceptually new and effective approach to designing and modulating the electronic and spatial environment around metal centers in organometallic compounds using a combination of multifunctional ligands and LBs/LAs.

Acknowledgments

We sincerely acknowledge all collaborators who contributed to the studies described herein. Ni K-edge XAS measurements were performed at the BL14B2 beamline of SPring-8 with the approval of the Japan Synchrotron Radiation Research Institute (proposal numbers 2020A1871, 2021A1630, 2021B1717, 2022A1767, and 2022A1784). Ni $L_{2,3}$-edge XAS measurements were performed at the BL-19B beamline of Photon Factory with the approval of the Photon Factory Program Advisory Committee (proposal number 2022P013) and at the BL4B beamline of the UVSOR Synchrotron Facility with the approval of the Institute for Molecular Science (proposal number 21-697). Part of the computational calculations was performed using resources of the Research Center for Computational Science, Okazaki, Japan (21-IMS-C105 and 22-IMS-C107).

Funding

We appreciate the financial support from Grants-in-Aid for Scientific Research (C) (JSPS KAKENHI Grant 21K05070 and 22K05095), for Young Scientists (JSPS KAKENHI Grant 20K15279), the Environment Research and Technology Development Fund (JPMEERF20211R01) of the Environmental Restoration and Conservation Agency of Japan, Transformative Research Area (A) Digitalization-driven Transformative Organic Synthesis (22H05363), JST FOREST Program (JPMJFR2222), a Mitsubishi Gas Chemical Award in Synthetic Organic Chemistry, and the RIKEN-Osaka University Science and Technology Hub Collaborative Research Program from RIKEN and Osaka University. A part of this work was supported by JST SPRING (Grant JPMJSP2138).

Conflict of interest statement. None declared.

References

1. K. Wu, A. G. Doyle, *Nat. Chem.* **2017**, *9*, 779. https://doi.org/10.1038/nchem.2741
2. L. Falivene, Z. Cao, A. Petta, L. Serra, A. Poater, R. Oliva, V. Scarano, L. Cavallo, *Nat. Chem.* **2019**, *11*, 872. https://doi.org/10.1038/s41557-019-0319-5
3. D. J. Durand, N. Fey, *Chem. Rev.* **2019**, *119*, 6561. https://doi.org/10.1021/acs.chemrev.8b00588
4. Z. Zhang, Y. Shao, J. Tang, J. Jiang, L. Wang, S. Li, *Green Synth. Catal.* **2021**, *2*, 156. https://doi.org/10.1016/j.gresc.2021.03.007
5. J. Trouvé, R. Gramage-Doria, *Chem. Soc. Rev.* **2021**, *50*, 3565. https://doi.org/10.1039/D0CS01339K
6. V. Blanco, D. A. Leigh, V. Marcos, *Chem. Soc. Rev.* **2015**, *44*, 5341 . https://doi.org/10.1039/C5CS00096C
7. A. J. M. Miller, *Dalton. Trans.* **2017**, *46*, 11987. https://doi.org/10.1039/C7DT02156A
8. C. Yoo, H. M. Dodge, A. J. M. Miller, *Chem. Commun.* **2019**, *55*, 5047. https://doi.org/10.1039/C9CC00803A
9. E. Peris, *Chem. Rev.* **2018**, *118*, 9988 . https://doi.org/10.1021/acs.chemrev.6b00695
10. C. J. Elsevier, J. Reedijk, P. H. Walton, M. D. Ward, *Dalton. Trans.* **2003**, 1896.
11. A. M. Allgeier, C. A. Mirkin, *Angew. Chem., Int. Ed.* **1998**, *37*, 894. https://doi.org/10.1002/(SICI)1521-3773(19980420)37:7<894::AID-ANIE894>3.0.CO;2-L
12. O. R. Luca, R. H. Crabtree, *Chem. Soc. Rev.* **2013**, *42*, 1440. https://doi.org/10.1039/C2CS35228A
13. B. M. Neilson, C. W. Bielawski, *ACS. Catal.* **2013**, *3*, 1874. https://doi.org/10.1021/cs4003673
14. R. Göstl, A. Senf, S. Hecht, *Chem. Soc. Rev.* **2014**, *43*, 1982. https://doi.org/10.1039/c3cs60383k
15. M. H. Shaw, J. Twilton, D. W. C. MacMillan, *J. Org. Chem.* **2016**, *81*, 6898. https://doi.org/10.1021/acs.joc.6b01449
16. R. H. Crabtree, *New J. Chem.* **2011**, *35*, 18. https://doi.org/10.1039/C0NJ00776E
17. S. Acosta-Calle, A. J. M. Miller, *Acc. Chem. Res.* **2023**, *56*, 971. https://doi.org/10.1021/acs.accounts.3c00056
18. G.-H. Ouyang, Y.-M. He, Y. Li, J.-F. Xiang, Q.-H. Fan, *Angew. Chem., Int. Ed.* **2015**, *54*, 4334. https://doi.org/10.1002/anie.201411593
19. T. Asada, Y. Hoshimoto, S. Ogoshi, *J. Am. Chem. Soc.* **2020**, *142*, 9772. https://doi.org/10.1021/jacs.0c03252
20. P. Braunstein, F. Naud, *Angew. Chem., Int. Ed.* **2001**, *40*, 680. https://doi.org/10.1002/1521-3773(20010216)40:4<680::aid-anie6800>3.0.co;2-0
21. C. Fliedel, G. Schnee, P. Braunstein, *Dalton. Trans.* **2009**, 2474. https://doi.org/10.1039/b902314n
22. Q. Liang, T. Janes, X. Gjergji, D. Song, *Dalton. Trans.* **2016**, *45*, 13872. https://doi.org/10.1039/C6DT02792J
23. M. Mondal, T. K. Ranjeesh, S. K. Gupta, J. Choudhury, *Dalton. Trans.* **2014**, *43*, 9356. https://doi.org/10.1039/c4dt00551a
24. Y. Yamauchi, Y. Hoshimoto, T. Kawakita, T. Kinoshita, Y. Uetake, H. Sakurai, S. Ogoshi, *J. Am. Chem. Soc.* **2022**, *144*, 8818. https://doi.org/10.1021/jacs.2c02870
25. Y. Hoshimoto, S. Ogoshi, *Bull. Chem. Soc. Jpn.* **2021**, *94*, 327. https://doi.org/10.1246/bcsj.20200293
26. S. Hazra, Y. Hoshimoto, S. Ogoshi, *Chem. Eur. J.* **2017**, *23*, 15238. https://doi.org/10.1002/chem.201703644
27. P. Nägele, U. Herrlich (neé Blumbach), F. Rominger, P. Hofmann, *Organometallics*. **2013**, *32*, 181. https://doi.org/10.1021/om300963t
28. W. Tao, S. Akita, R. Nakano, S. Ito, Y. Hoshimoto, S. Ogoshi, K. Nozaki, *Chem. Commun.* **2017**, *53*, 2630. https://doi.org/10.1039/C7CC00002B
29. L. P. Spencer, M. D. Fryzuk, *J. Organomet. Chem.* **2005**, *690*, 5788. https://doi.org/10.1016/j.jorganchem.2005.07.121
30. C. Fliedel, P. Braunstein, *Organometallics*. **2010**, *29*, 5614. https://doi.org/10.1021/om100500y
31. A. J. Arduengo III, J. S. Dolphin, G. Gurău, W. J. Marshall, J. C. Nelson, V. A. Petrov, J. W. Runyon, *Angew. Chem., Int. Ed.* **2013**, *52*, 5110. https://doi.org/10.1002/anie.201301503
32. L. Branzi, M. Baron, L. Armelao, M. Rancan, P. Sgarbossa, C. Graiff, A. Pöthig, A. Biffis, *New J. Chem.* **2019**, *43*, 17275. https://doi.org/10.1039/C9NJ04911H
33. Y. Yamauchi, Y. Mondori, Y. Uetake, Y. Takeichi, T. Kawakita, H. Sakurai, S. Ogoshi, Y. Hoshimoto, *J. Am. Chem. Soc.* **2023**, *145*, 16938. https://doi.org/10.1021/jacs.3c06267
34. H.-W. Häring, *Industrial Gases Processing*, Wiley–VCH, Weinheim, **2008**.
35. ÁA Ramírez-Santos, C. Castel, E. Favre, *Sep. Purif. Technol.* **2018**, *194*, 425. https://doi.org/10.1016/j.seppur.2017.11.063

Downloaded from https://academic.oup.com/chemlett/article/53/3/upae042/7623711 by USACO ref BMB 39121 user on 06 December 2024

36. L. Mond, C. Langer, F. L. Quincke, *J. Chem. Soc., Trans*. **1890**, *57*, 749. https://doi.org/10.1039/CT8905700749
37. A. Morrison, J. J. Leitch, G. Szymanski, G. Moula, B. Barlow, I. J. Burgess, B. Shobeir, H. Huang, J. Lipkowski, *Electrochim. Acta*. **2018**, *260*, 684. https://doi.org/10.1016/j.electacta.2017.12.016
38. L. S. Sunderlin, D. Wang, R. R. Squires, *J. Am. Chem. Soc*. **1992**, *114*, 2788. https://doi.org/10.1021/ja00034a004
39. M. Zhou, L. Andrews, C. W. Bauschlicher Jr, *Chem. Rev*. **2001**, *101*, 1931. https://doi.org/10.1021/cr990102b
40. J. N. Leung, Y. Mondori, S. Ogoshi, Y. Hoshimoto, H. V. Huynh, *Inorg. Chem*. **2024**, *63*, 4344. https://doi.org/10.1021/acs.inorgchem.3c04600
41. R. Dorta, E. D. Stevens, N. M. Scott, C. Costabile, L. Cavallo, C. D. Hoff, S. P. Nolan, *J. Am. Chem. Soc*. **2005**, *127*, 2485. https://doi.org/10.1021/ja0438821
42. R. Dorta, E. D. Stevens, C. D. Hoff, S. P. Nolan, *J. Am. Chem. Soc*. **2003**, *125*, 10490. https://doi.org/10.1021/ja0362151
43. A. Levina, R. S. Armstrong, P. A. Lay, *Coord. Chem. Rev*. **2005**, *249*, 141. https://doi.org/10.1016/j.ccr.2004.10.008
44. S. Gross, M. Bauer, *Adv. Funct. Mater*. **2010**, *20*, 4026. https://doi.org/10.1002/adfm.201000095
45. S. Bordiga, E. Groppo, G. Agostini, J. A. van Bokhoven, C. Lamberti, *Chem. Rev*. **2013**, *113*, 1736. https://doi.org/10.1021/cr2000898
46. J. K. Kowalska, F. A. Lima, C. J. Pollock, J. A. Rees, S. DeBeer, *Isr. J. Chem*. **2016**, *56*, 803. https://doi.org/10.1002/ijch.201600037
47. J. Timoshenko, B. R. Cuenya, *Chem. Rev*. **2021**, *121*, 882. https://doi.org/10.1021/acs.chemrev.0c00396
48. B. R. Stults, R. M. Friedman, K. Koenig, W. Knowles, R. B. Greegor, F. W. Lytle, *J. Am. Chem. Soc*. **1981**, *103*, 3235. https://doi.org/10.1021/ja00401a063
49. A. S. K. Hashmi, C. Lothschütz, M. Ackermann, R. Doepp, S. Anantharaman, B. Marchetti, H. Bertagnolli, F. Rominger, *Chem.-Eur. J*. **2010**, *16*, 8012. https://doi.org/10.1002/chem.200903450
50. M. Tromp, G. P. F. van Strijdonck, S. S. van Berkel, A. van den Hoogenband, M. C. Feiters, B. de Bruin, S. G. Fiddy, A. M. J. van der Eerden, J. A. van Bokhoven, P. W. N. M. van Leeuwen, D. C. Koningsberger, *Organometallics*. **2010**, *29*, 3085. https://doi.org/10.1021/om9010643
51. E. Bayram, J. C. Linehan, J. L. Fulton, J. A. S. Roberts, N. K. Szymczak, T. D. Smurthwaite, S. Özkar, M. Balasubramanian, R. G. Finke, *J. Am. Chem. Soc*. **2011**, *133*, 18889. https://doi.org/10.1021/ja2073438
52. H. Asakura, T. Shishido, T. Tanaka, *J. Phys. Chem. A*. **2012**, *116*, 4029. https://doi.org/10.1021/jp211627v
53. K. P. Kornecki, J. F. Briones, V. Boyarskikh, F. Fullilove, J. Autschbach, K. E. Schrote, K. M. Lancaster, H. M. L. Davies, J. F. Berry, *Science*. **2013**, *342*, 351. https://doi.org/10.1126/science.1243200
54. C. He, G. Zhang, J. Ke, H. Zhang, J. T. Miller, A. J. Kropf, A. Lei, *J. Am. Chem. Soc*. **2013**, *135*, 488. https://doi.org/10.1021/ja310111p
55. R. Schoch, W. Desens, T. Werner, M. Bauer, *Chem.-Eur. J*. **2013**, *19*, 15816. https://doi.org/10.1002/chem.201303340
56. H. Takaya, S. Nakajima, N. Nakagawa, K. Isozaki, T. Iwamoto, R. Imayoshi, N. J. Gower, L. Adak, T. Hatakeyama, T. Honma, M. Takagaki, Y. Sunada, H. Nagashima, D. Hashizume, O. Takahashi, M. Nakamura, *Bull. Chem. Soc. Jpn*. **2015**, *88*, 410. https://doi.org/10.1246/bcsj.20140376
57. K. Nomura, T. Mitsudome, A. Igarashi, G. Nagai, K. Tsutsumi, T. Ina, T. Omiya, H. Takaya, S. Yamazoe, *Organometallics*. **2017**, *36*, 530. https://doi.org/10.1021/acs.organomet.6b00727
58. M. Hirano, K. Sano, Y. Kanazawa, N. Komine, Z. Maeno, T. Mitsudome, H. Takaya, *ACS. Catal*. **2018**, *8*, 5827. https://doi.org/10.1021/acscatal.8b01095
59. T. Niwa, Y. Uetake, M. Isoda, T. Takimoto, M. Nakaoka, D. Hashizume, H. Sakurai, T. Hosoya, *Nat. Catal*. **2021**, *4*, 1080. https://doi.org/10.1038/s41929-021-00719-6
60. A. Yamamoto, X. Liu, K. Arashiba, A. Konomi, H. Tanaka, K. Yoshizawa, Y. Nishibayashi, H. Yoshida, *Inorg. Chem*. **2023**, *62*, 5348. https://doi.org/10.1021/acs.inorgchem.2c03752
61. A. Gómez-Suárez, D. J. Nelson, S. P. Nolan, *Chem. Commun*. **2017**, *53*, 2650. https://doi.org/10.1039/C7CC00255F

Downloaded from https://academic.oup.com/chemlett/article/53/3/upae042/7623711 by USACO ref BMB 39121 user on 06 December 2024